Deciphering site-specific histopathological parameters with potential clinical value in head and neck squamous cell carcinomas

SOFIA-ELENI TZORAKOLEFTHERAKI[1], VASSILIKI KOTOULA[1], GEORGIOS KARAKATSOULIS[2], KONSTANTINOS MARKOU[3], STAVROULA PERVANA[4], KONSTANTINOS VLACHTSIS[5], SOFIA CHRISAFI[6], AMANDA PSYRRI[7], GEORGE FOUNTZILAS[6,8], PRODROMOS HYTIROGLOU[1] and TRIANTAFYLLIA KOLETSA[1]

[1]Department of Pathology, Aristotle University of Thessaloniki, School of Health Sciences, Faculty of Medicine, 54124 Thessaloniki, Greece; [2]Institute of Applied Biosciences, Centre for Research and Technology Hellas, 57001 Thessaloniki, Greece; [3]Department of Otorhinolaryngology, Papageorgiou Hospital, Aristotle University of Thessaloniki, 56403 Thessaloniki, Greece; [4]Department of Pathology, Papageorgiou Hospital, 56403 Thessaloniki, Greece; [5]First Department of Otorhinolaryngology, Papanikolaou Hospital, 57010 Thessaloniki, Greece; [6]Laboratory of Molecular Oncology, Hellenic Foundation for Cancer Research/Aristotle University of Thessaloniki, 54124 Thessaloniki, Greece; [7]Section of Medical Oncology, Department of Internal Medicine, Attikon University Hospital, Faculty of Medicine, National and Kapodistrian University of Athens School of Medicine, 12462 Athens, Greece; [8]Aristotle University of Thessaloniki, 54124 Thessaloniki, Greece

Received May 9, 2025; Accepted September 8, 2025

DOI: 10.3892/ol.2025.15315

Abstract. In the diagnostic setting of head and neck squamous cell carcinoma (HNSCC), there is an unmet need for robust histological prognosticators, since grading alone is considered to be of disputed clinical relevance. In this context, the present study assessed site-specific and tumor compartment characteristics as potential histological risk factors in HNSCC. Morphological and immunophenotypic (such as CD8 and PD-L1) characteristics of tumor cells, the immune microenvironment and the invasive margin (IM) were assessed in 248 patients with HNSCC who were followed up for >20 years, to determine their site specificity and impact on the overall survival of patients. Laryngeal and hypopharyngeal carcinomas were characterized by keratinization, cell cannibalism and anaplastic features; oropharyngeal carcinoma was characterized by a high grade and necrosis; and oral carcinomas was characterized by keratin pearls, eosinophil infiltrates and perineural invasion (P<0.05). CD8 distribution homogeneity, tumor center and/or IM perineural invasion, and sparse lymphocytic host response in the IM (LHR-IM) were unfavorable prognosticators (P<0.05). Among these parameters, only LHR-IM and perineural invasion throughout the tumor independently predicted an unfavorable prognosis, along with disease stage. Grade, keratinization, anaplastic features, cell cannibalism, necrosis-related features, eosinophils, worst pattern of invasion (the most aggressive pattern of tumor cell proliferation found at the invasive front), tumor lymphocytic and $CD8^+$ T-cell infiltrates, and primary site were not associated with prognosis in the present study. In conclusion, perineural invasion and LHR-IM were confirmed as histological risk factors in HNSCC, which should be included in pathology reports. To revise the assessment of HNSCC tumor grade, the aforementioned site-specific histological characteristics may be used in deep learning algorithms.

Correspondence to: Dr Sofia-Eleni Tzorakoleftheraki, Department of Pathology, Aristotle University of Thessaloniki, School of Health Sciences, Faculty of Medicine, University Campus, 54124 Thessaloniki, Greece
E-mail: stzorako@auth.gr

Abbreviations: HeCOG, Hellenic Cooperative Oncology Group; H&E, hematoxylin & eosin; HNSCC, head and neck squamous cell carcinoma; HPV, human papilloma virus; IM, invasive margin; IQR, interquartile range; LHR, lymphocytic host response; OS, overall survival; PNI, perineural invasion; SCC, squamous cell carcinoma; TIL, tumor infiltrating lymphocyte; TMA, tissue microarray

Key words: invasive margin, heterogeneity, tumor microenvironment, cell cannibalism, histologic grade

Introduction

Head and neck carcinoma accounts for 4.6% of all cancers worldwide, and there has been an annual 1.4-fold increase in the number of new cases per year during the last decade (1,2). Squamous cell carcinomas (SCC) comprise the most common type of malignancy in this wide anatomical region, which includes the oral cavity, pharynx, and larynx (3). Although tobacco smoke and alcohol consumption are traditionally considered major risk factors for head and neck SCC (HNSCC), viruses are also accountable (4). Two types of viruses, namely, Human Papilloma Virus (HPV) and Epstein-Barr Virus, are strongly associated with oropharyngeal and nasopharyngeal SCC, respectively, since virus-associated carcinomas exhibit a predilection for sites with lymphoid-based mucosa (3,5). In fact, according to the latest recommendations of The College of American Pathologists, all newly diagnosed oropharyngeal

SCC should be examined by immunohistochemistry, using p16 as a surrogate marker for potential HPV infection (6), while HPV-related oropharyngeal cancer is currently considered as a unique disease entity in both the pathological (7) and clinical (8) context. Emerging molecular drivers such as lncRNA BLACAT1 have been implicated in adjacent sites like hypopharyngeal SCC (9), underscoring the need to integrate morphologic and transcriptomic data in future studies. Epigenetic dysregulation is a common feature across cancers; chromatin-remodeling complex vulnerabilities may provide novel therapeutic targets in HNSCC, as recently suggested for a different type of tumors (10).

Several studies have reported the significance of both tumor cells and tumor microenvironment histopathological characteristics in HNSCC. Emerging data have highlighted the importance of phenotypic heterogeneity in these carcinomas and its role in the development and progression of the tumors as well as in treatment efficacy (11). In this context, the prognostic value of traditional grading is debatable, whereas other histopathological features, i.e. worst pattern of invasion and intensity of lymphocytic infiltration in the invasive margin of HNSCC, seem directly associated with patient overall survival (OS) (12,13).

In the present study, we assessed histopathological parameters of tumor cells and their microenvironment in tumor compartments (center and invasive margin) of HNSCC originating in different anatomical sites. We evaluated these parameters against each other and against clinicopathological characteristics of the patients to identify potential risk factors with clinical relevance.

Materials and methods

Tissue samples and patient data. Formalin-fixed paraffin-embedded tissue samples from patients with histologically confirmed HNSCC and available clinical, histopathological, treatment, and outcome data were retrieved from the Hellenic Cooperative Oncology Group (HeCOG) clinical database and biologic material repository. Since nasopharyngeal carcinoma is generally considered a biologically different disease compared to SCC of the rest of the head and neck region, especially in Far East and Mediterranean basin, we explored this neoplasm separately on genomic, histopathological and clinical basis (14-16) and it was excluded from this study. In the same line, p16 positive HNSCC considered as HPV-related, which are biologically different from other HNSCC (7), were excluded, as well. Patients with HNSCC were diagnosed and treated between 1999 and 2018. Written informed consent was obtained from all patients for the use of their data and biologic material for research purposes. The protocol was approved by the Bioethics Committee of the Aristotle University of Thessaloniki, School of Health Sciences, Faculty of Medicine (approval no. 5/18.12.2019; Thessaloniki, Greece).

New Hematoxylin and Eosin (H&E) sections from all tissue blocks were reviewed for histological evaluation and tumor tissue adequacy (tumor cells and stroma). The tumor surface area was separated into tumor center and invasive margin according to the literature (17,18). As such, the invasive margin was defined as the region around the border where normal tissue meets malignant cells, extending by 1 millimeter. Samples from advanced HNSCC that were not obtained from the primary site (e.g., metastatic lymph nodes) or where a primary site could not be determined, were annotated as 'local spread'. Based on the availability of clinical data and adequate tumor tissue, 248 tumors from the same number of patients were examined. Patient age at first diagnosis ranged from 20.9 to 85.1 years, with a median of 62 years.

Histological evaluation. Parameters assessed on whole H&E sections were: i) Keratinization (present/absent). Tumors exhibiting squamous maturation features on less than 10% of their surface were not classified as keratinizing (19); ii) area occupied by keratin pearls as percentage of the entire tumor area; iii) presence of specific spatial distribution of neutrophils, that is, neutrophils in tumor necrotic areas and in close proximity to dyskeratotic cells, as well as microabscesses in keratinization; iv) histologic grading, according to the three-tier grading system (G1, G2, G3) (20); v) extent of tumor necrosis, as absent, focal (≤10% of the tumor area), moderate (11-29% of the tumor area), or extensive (≥30% of the tumor area) (21); and the presence of necrosis in keratinization areas. However, since only one case exhibited extensive necrosis, it was included in the moderate group; vi) anaplastic cells defined as cells with lack of differentiation, showing pleomorphism, nuclear abnormalities, atypical mitoses and loss of polarity (present/absent) (22); vii) cell cannibalism, which corresponds to cell-in-cell phenomenon, a process of non-apoptotic cell death, where one cancer cell surrounds another cancer cell (present/absent) (23); viii) tumor stroma classification, as myxoid, when there was an amorphous stromal substance comprising of slightly basophilic extracellular matrix; as keloid-like, regulated by specific channels (24), when thick bundles of hypocellular collagen with bright eosinophilic hyalinization were evident; or as fibroblastic, when only fine mature collagen fibers were evident (25); ix) tumor infiltrating lymphocyte (TIL) density; according to international guidelines (17,26), ten high-power fields of each section excluding pre-existing lymphoid background areas (17,27), were assessed, and the mean average was estimated; and x) perineural and lymphovascular invasion (present/absent). The presence of calcification and giant cell reaction was also recorded.

Eosinophil number per mm^2 was evaluated similarly to $CD8^+$ counts on Tissue MicroArray (TMA) sections (28).

Histological parameters in the invasive margin were examined separately, based on previous studies (5,12,13,29): keratinization was assessed as absent (0-5% of the invasive margin area), low (6-20%), moderate (21-50%), and high (>50%); cellular atypia and pleomorphism were estimated as mild, moderate, and severe; mature squamous cells with angular shape, eosinophilic cytoplasm, and intercellular bridges were recorded in a four-tier scale, based on their abundance (0-25%, 26-50%, 51-75%, and >75%); lymphocytic host response along the invasive margin was recorded as dense (dense lymphocytic response rimming the tumor and/or lymphoid nodules at advancing edge in each 4x field), intermediate (intermediate lymphocytic response and/or lymphoid nodules in some but not all 4x fields), and weak (sparse lymphocytic response without lymphoid nodules) (13); and perineural invasion was assessed separately in this tumor compartment. The worst pattern of invasion, defined as the least differentiated part

of the invasive margin of tumors, included five categories, namely, pushing border, finger-like growth, large tumor islands (>15 cells/island), small tumor islands (<15 cells/island), and tumor satellites ≥1 mm away from the main tumor.

Immunohistochemistry. Immunohistochemistry was performed on 3-μm TMA sections. To confirm HPV-negative status, $p16^{INK4A}$ mouse monoclonal antibody (clone IHC116, GenomeMe, Lab Inc., Richmond, BC, Canada) was applied at 1:50 dilution, on a Bond Max Autostainer using BOND Polymer Detection kit. Antigen retrieval was performed with EDTA (pH 9) for 40 min, followed by primary antibody ($p16^{INK4A}$) incubation at 37˚C for 30 min. For immune profiling, CD8 mouse monoclonal antibody (clone C8/144B, Dako, Glostrup, Denmark) was used at 1:60 dilution. For antigen retrieval, EDTA (pH 9) was used for 20 min, before primary antibody incubation at 37˚C for 30 min. Staining was performed on a Dako autostainer using the EnVision™ FLEX+ (Agilent, Santa Clara, CA) visualization system. PD-L1 was assessed with a mouse monoclonal antibody (clone 22C3, Dako, Glostrup, Denmark) at 1:100 dilution on a Dako autostainer by using the EnVision™ FLEX+ visualization system (Agilent, Santa Clara, CA). For antigen retrieval, EDTA (pH 9) was performed for 30 min, followed by primary antibody incubation at 37˚C for 30 min. All slides were counterstained with hematoxylin. Both positive and negative controls were simultaneously stained.

In regard to immunohistochemical evaluation, PD-L1 expression was assessed in both tumor and immune cells, according to the guidelines (30). For tumor cells, PD-L1 positivity was defined as complete and/or partial circumferential linear cellular membrane staining of any intensity, as assessed by the tumor proportion score (TPS). Immune cells were evaluated as the proportion of the tumor area occupied by any discernible PD-L1 staining of any intensity and the combined positive score (CPS) was estimated in each case (30). CPS ≥1 was considered positive. Staining interpretation was performed by two experienced pathologists (SET, TK). $CD8^+$ cell counts were obtained from the entire area of each 1.5 mm diameter core. The density of positive cells was assessed as the ratio of $CD8^+$ cells per mm^2 of core surface area. Average values were used for tumors represented by multiple cores. Spatial distribution of $CD8^+$ T cells was assessed by comparing two tissue cores of each tumor to determine whether cells were evenly distributed, clustered or concentrated in specific regions or showed different values between the cores (28). For p16, strong and diffuse nuclear and/or cytoplasmic positivity in ≥70% of neoplastic cells was used as a cut-off according to standard guidelines for HNSCC, with a positive result indicating HPV-related HNSCC (31). As aforementioned, p16 immunohistochemistry (Fig. S1) was applied to all available HNSCC cases and HPV-related carcinomas were excluded from the present study; accordingly, all tumors analyzed here were p16 negative.

Statistical analysis. Histological parameters, categorical and continuous, were evaluated against clinicopathological patient and tumor characteristics and against each other. In case of two categorical variables χ^2 and Fisher's tests were applied. In case of comparing a continuous variable across different groups, the Kruskal-Wallis(if more than two groups) and the Mann-Whitney (if two groups) tests were used. In case of post hoc comparisons, Kruskal Wallis test, followed by Mann-Whitney U test and Bonferroni correction was applied.

For the assessment of risk factors for OS, the log-rank test and Cox regression were applied. For multivariable analyses, we selected risk factors with a P-value lower than 0.2, which were further filtered by using Akaike's information criterion for entry into the multivariable model.

The significance level for univariable analyses was set at 5%, with $P<0.05$ considered to indicate a statistically significant difference. All analyses were conducted in R (v. 4.3.1; https://www.R-project.org/).

Results

Patient and tumor characteristics. Most patients were men, heavy smokers, and diagnosed with stage III or IV disease. The majority underwent surgical treatment, while 26.25% received various therapeutic modalities in the first line setting. Based on tumor location as per histopathology report, SCC were categorized into oral, oropharyngeal, hypopharyngeal, and laryngeal, the two latter categories being analyzed as one. Twenty-seven cases of local spread specimens were incorporated in the study. Most tumor tissues were obtained at disease diagnosis and were surgical specimens. Seventy-nine of them included the invasive margin of the tumor. The resection margins were free of carcinoma/high grade dysplasia. All available clinicopathological data are presented in Table I.

Phenotype characteristics. Detailed histopathological and immunophenotypic characteristics of the examined HNSCC are shown in Table II.

The most prevalent tumor variant was keratinizing of intermediate grade (G2) with anaplastic features and cell cannibalism (Fig. 1A). Among the laryngeal SCC, two were designated as basaloid SCC variants. Two additional basaloid SCC were found; one located in the oral cavity and one in the oropharynx. Neutrophils in dyskeratosis (Fig. 1B) were quite common, whereas keratin pearls in ≥5% of the tumor area, microabscesses, or necrosis in keratinization (Fig. 1C) were observed in a minority of tumors. Perineural and lymphovascular invasion were rare. Grade (Fig. 1D and E) heterogeneity was observed in a considerable number of tumors. Specifically, while most of them presented with intermediate grade (G2), 'miniscule' areas with features favoring either low (G1) or high (G3) grade frequently coexisted. In all cases with grading heterogeneity, the final grade was assigned based on the worst component, if it comprised more than 5%. Accordingly, stromal desmoplastic reaction presented with a variety of features, from loose myxoid to dense collagenous, even within the same tumor, in respect of stromal heterogeneity. In such cases, stroma was characterized based on the predominant pattern.

The infiltrative margin in 63 (79.7%) out of 79 evaluable tumors was characterized by the absence of keratinization. In the same tumor area, heterogeneous worst pattern of invasion was identified in 32/79 cases (40.5%) (Fig. 1F); all degrees of lymphocytic host response density were equally observed, while perineural invasion (Fig. 1G) was noticed in 11.4% of the tumors.

Table I. Head and neck squamous cell carcinoma patient demographics and clinicopathological data.

Characteristic	Value
Median age at first diagnosis, years (IQR min-max; range)	62 (54.23-70.1; 20.9-85.1)
Sex (n=248)	
Female	31 (12.5)
Male	217 (87.5)
Smoking packs (n=225)	
No	25 (11.1)
1-10 pack years	9 (4.0)
11-20 pack years	27 (12.0)
>20 pack years	164 (72.9)
Alcohol abuse (n=226)	
No	68 (30.1)
Mild	53 (23.5)
Moderate	41 (18.1)
Heavy	64 (28.3)
Disease stage (n=229)[a]	
I	25 (10.9)
II	27 (11.8)
III	65 (28.4)
IV	112 (48.9)
Adjuvant treatment (n=242)	
No	210 (86.8)
Chemo	1 (0.4)
RT	31 (12.8)
First line treatment (n=240)	
No	177 (73.8)
Chemo	38 (15.8)
CT-RT	7 (2.9)
RT	18 (7.5)
Death (n=246)	
No	59 (24.0)
Yes	187 (76.0)
Tumor site (n=248)	
Oral	35 (14.1)
Oropharyngeal	30 (12.1)
Laryngohypopharyngeal	156 (62.9)
Local spread[b]	27 (10.9)
Sample status (n=242)	
First diagnosis	202 (83.5)
Pretreated[c]	23 (9.5)
Relapse, naïve[d]	17 (7.0)
Type of specimen (n=248)	
Biopsy	78 (31.5)
Surgical	170 (68.5)

Data are presented as n (%), unless otherwise indicated. [a]Stage was pooled into the main 4 categories according to AJCC 8th ed; [b]tumor spread to adjacent anatomical structures and/or lymph nodes; [c]radiotherapy +/- chemotherapy; [d]preceding surgical treatment only. RT, radiotherapy; chemo, chemotherapy; CT-RT, chemotherapy and radiotherapy; IQR, interquartile range.

Table II. Histopathological and immunohistochemical characteristics of head and neck squamous cell carcinoma cases.

Characteristic	Value
Grade (n=248)	
G1	42 (16.9)
G2	155 (62.5)
G3	51 (20.6)
Grade heterogeneity (n=248)	24 (9.7)
Tumor variant (n=248)	
Keratinizing	196 (79.0)
Non keratinizing	52 (21.0)
Anaplastic features (n=248)	138 (55.6)
Cell cannibalism (n=248)	139 (56.0)
Desmoplastic stromal reaction (n=222)	
Fibroblastic	134 (60.4)
Keloid-like	27 (12.1)
Loose/myxoid	61 (27.5)
Stromal reaction heterogeneity (n=222)	37 (16.7)
Necrosis[a] (n=248)	
Absent	220 (88.7)
Focal	21 (8.5)
Moderate-extensive	7 (2.8)
Microabscesses (n=248)	13 (5.2)
Necrosis in keratinization (n=248)	68 (27.4)
Neutrophils in necrosis (n=248)	14 (5.6)
Neutrophils in dyskeratosis (n=248)	126 (50.8)
Perineural invasion[b] (n=248)	12 (4.8)
Lymphovascular invasion (n=248)	4 (1.6)
CD8 heterogeneity (n=159)	41 (25.8)
PD-L1 status (n=215)	
<1	190 (88.4)
1-20	22 (10.2)
≥20	3 (1.4)
PD-L1 heterogeneity (n=215)	12 (5.6)
Lymphocytic host response in IM (n=79)	
Weak	28 (35.4)
Intermediate	27 (34.2)
Dense	24 (30.4)
Perineural invasion in IM (n=79)	9 (11.4)
Multinucleated macrophages (n=248)	29 (11.7)
Median keratin pearls[a] (n=248) [IQR]	0 [0, 5]
Median eosinophils/mm^2 (n=214) [IQR]	0.314 [0, 3.88]
Median TIL Salgado density (n=242) [IQR]	20.75 [11.15, 32.35]
Median CD8$^+$/mm^2 (n=215) [IQR]	198.05 [98.45, 420.37]

Data are presented as n (%), unless otherwise indicated. [a]% of tumor surface; [b]assessed in the entire tumor area. IM, invasive margin; IQR, interquartile range.

With respect to immune cell infiltrates, 10.3% of tumors exhibited eosinophils >14.2/mm^2, while 15% of tumors

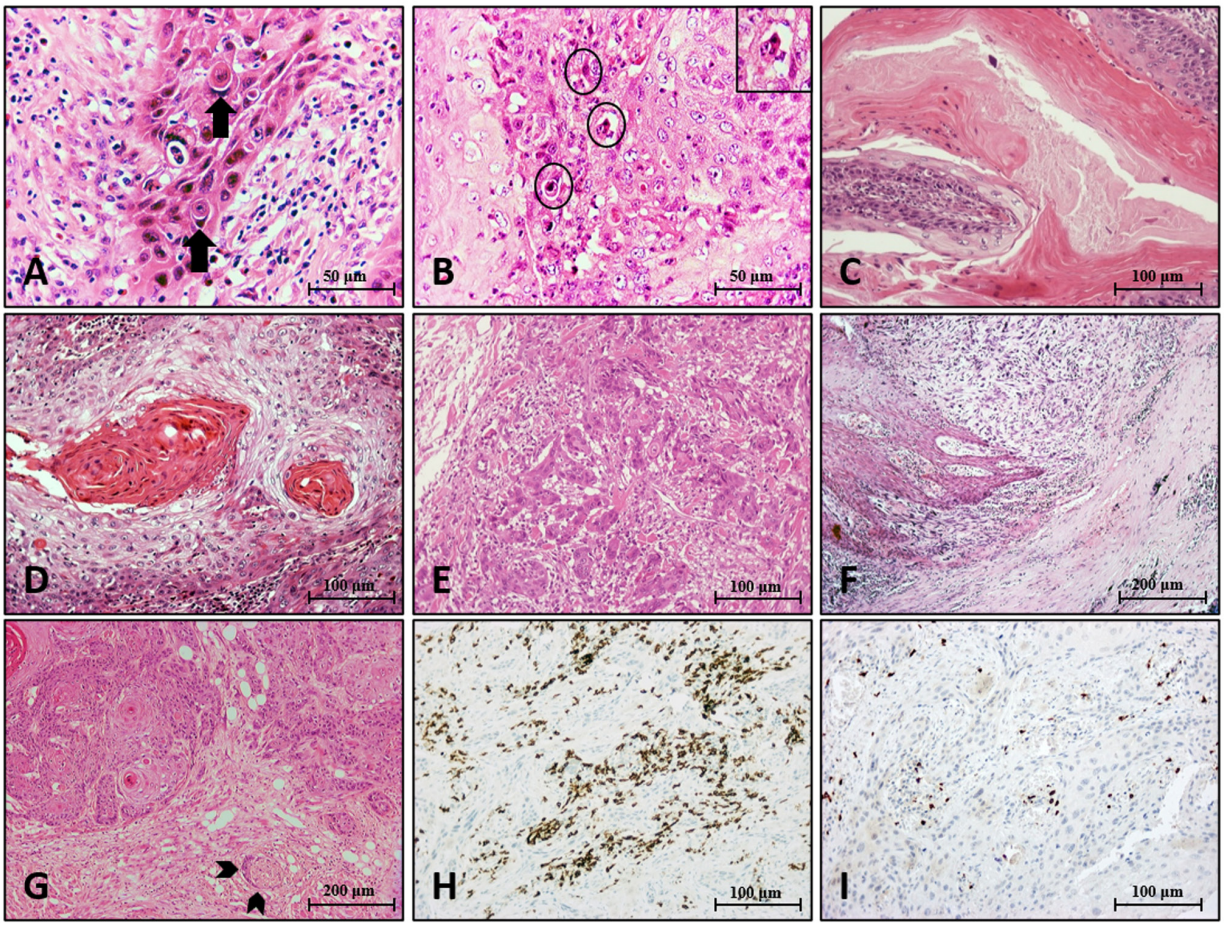

Figure 1. Histopathological features of HNSCC cases: (A) Cell-in-cell structures (arrows) in a case of laryngeal carcinoma (H&E x400). (B) Neutrophils in dyskeratosis (encircled)/inset: neutrophils in close proximity to dyskeratotic cell in a case of laryngeal carcinoma (H&E x400). (C) Necrosis in keratinization in a case of laryngeal carcinoma (H&E x200); Grading heterogeneity with (D) well differentiated and (E) moderately differentiated areas within a single case of laryngeal carcinoma (H&E x200; H&E x200). (F) Multiple worst patterns of invasion along the invasive margin within the same case of oral carcinoma (H&E x100). (G) Perineural invasion in the invasive margin of an oral carcinoma (H&E x100). Heterogeneity in T8 lymphocytic density in an oropharyngeal case presenting (H) abundant $CD8^+$ T cells in one tissue core of the tumor, and (I) only a few in the other (CD8 x200). HNSCC, head and neck squamous cell carcinoma.

had TIL density >50% and/or $CD8^+$ >700/mm^2. $CD8^+$ infiltrates were heterogeneously present in 25.8% of the tumors (Fig. 1H and I). Only 11.6% exhibited any degree of PD-L1 positivity (Fig. S1).

Site specificity of generic histopathological characteristics. Histological characteristics significantly differed among HNSCC from different anatomical areas, namely, laryngohypopharyngeal, oropharyngeal, and oral carcinomas, as shown in Table III. Regarding some of these characteristics, the majority of laryngohypopharyngeal tumors exhibited anaplastic features and cell cannibalism. Oropharyngeal tumors featured higher grade and higher rates of tumor necrosis, while being devoid of eosinophils. In contrast, eosinophils, keratin pearls, and perineural invasion were more common in oral carcinomas. In addition, keratinization was prevalent among laryngohypopharyngeal tumors (P<0.001). Regarding the invasive margin (Table III), perineural invasion appeared more frequently in oral and oropharyngeal tumors.

Next, we profiled histological parameters for all tumors (Fig. 2). By definition, parameters related to keratinization were identified at significantly higher rates in keratinizing tumors (grade and necrosis in keratinization, neutrophils in dyskeratosis; all P-values <0.001). In comparison, anaplastic features, cell cannibalism and perineural invasion were almost equally distributed among tumors with and without keratinization. Modeling parameters related and not related to keratinization revealed a site-specific association; that is, concomitant keratinization and cell cannibalism were rare among oral and oropharyngeal tumors (P<0.001) (Table III). With respect to clinical parameters, laryngohypopharyngeal and oropharyngeal carcinomas were more frequent in heavy smokers (P=0.009) and in patients with stage III and IV disease (P=0.009). No further clinicopathological associations were observed.

No associations with tumor site were found for worst pattern of invasion and lymphocytic host response in the invasive margin. Similarly, there were no associations for tumor variant, tumor necrosis, neutrophils in necrosis or in dyskeratosis, microabscesses, stromal reaction, lymphovascular invasion, multinucleated macrophages, CD8 and PD-L1 status.

Associations between clinicopathological parameters and survival. All parameters were examined for their association

Table III. Associations between clinicopathological variables and tumor site.

Parameter	Oral	Oropharyngeal	Laryngo-hypopharyngeal	P-value
Smoking packs, n (%)				0.009
No	6 (24%)	2 (8.3%)	17 (11.1%)	
1-10	4 (16%)	2 (8.3%)	3 (2%)	
11-20	4 (16%)	2 (8.3%)	20 (13.1%)	
>20	11 (44%)	18 (75.1%)	113 (73.8%)	
Disease stage				0.009
I	8 (28.6%)	0 (0%)	15 (9.9%)	
II	4 (14.3%)	4 (16%)	19 (12.5%)	
III	3 (10.7%)	6 (24%)	53 (34.9%)	
IV	13 (46.4%)	15 (60%)	65 (42.7%)	
Grade				0.002
G1	12 (34.3%)	4 (13.3%)	23 (14.7%)	
G2	21 (60%)	15 (50%)	106 (68%)	
G3	2 (5.7%)	11 (36.7%)	27 (17.3%)	
Necrosis in keratinization				<0.001
Absent	34 (97.1%)	27 (90%)	97 (62.2%)	
Present	1 (2.9%)	3 (10%)	59 (37.8%)	
Anaplastic features				0.006
Absent	21 (60%)	17 (56.7%)	55 (35.3%)	
Present	14 (40%)	13 (43.3%)	101 (64.7%)	
Cell cannibalism				<0.001
Absent	25 (71.4%)	18 (60%)	52 (33.3%)	
Present	10 (28.6%)	12 (40%)	104 (66.7%)	
Perineural invasion (entire tumor area)				0.004
Absent	29 (82.9%)	28 (93.3%)	152 (97.4%)	
Present	6 (17.1%)	2 (6.7%)	4 (2.6%)	
Perineural invasion (invasive margin)				0.004
Absent	11 (64.7%)	0 (0%)	59 (96.7%)	
Present	6 (35.3%)	1 (100%)	2 (3.3%)	
Tumor variant and cell cannibalism status				<0.001
Keratinizing without cell cannibalism	20 (26.3%)	13 (17.1%)	43 (56.6%)	
Non keratinizing without cell cannibalism	5 (26.3%)	5 (26.3%)	9 (47.4%)	
Keratinizing with cell cannibalism	9 (8.8%)	7 (6.9%)	86 (84.3%)	
Non keratinizing with cell cannibalism	1 (4.2%)	5 (20.8%)	18 (75%)	
Median keratin pearls, % of tumor surface (IQR)	6.31 (8.64)	3.13 (6.33)	5.81 (12.92)	0.034
Median TIL density, % (IQR)	22.53 (12.39)	30.26 (20.71)	23 (16.3)	0.265
Median $CD8^+/mm^2$ (IQR)	395.63 (365.59)	305.74 (269.88)	273.58 (281.18)	0.123
Median eosinophils/mm^2 (IQR)	15.99 (29.16)	2.57 (5.09)	13.51 (74.71)	0.003

IQR, interquartile range.

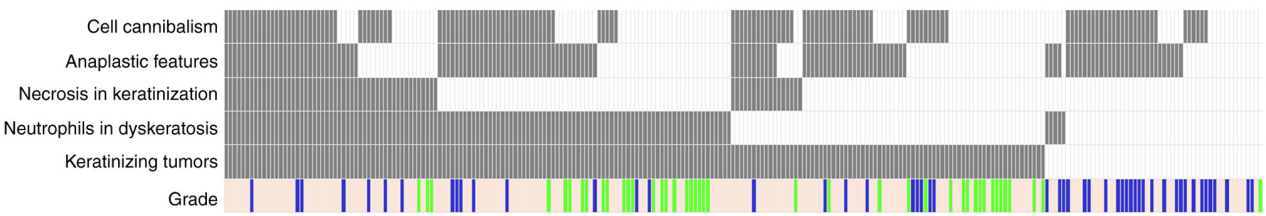

Figure 2. Profile map of histological parameters focused on keratinization. Grade 1, green; grade 2, pink; grade 3, dark blue.

Table IV. Univariable analysis with respect to OS for the parameters studied in the entire cohort and in the invasive margin.

A, Entire cohort

Parameter	Cases	Events	HR	95% CI	P-value
Sex					0.102
Female	30	17	1	-	
Male	216	164	1.51	(0.92, 2.49)	
Smoking					0.264
No	25	20	1	-	
Yes	200	147	0.76	(0.47, 1.23)	
Smoking pack years; only smokers			1.03	(0.88, 1.22)	0.077
Alcohol abuse					<0.001
No	68	44	1	-	
Mild	53	34	0.93	(0.59, 1.46)	
Moderate	41	31	1.44	(0.91, 2.28)	
Heavy	64	58	2.60	(1.73, 3.89)	
Disease stage					<0.001
I	25	13	1	-	
II	25	17	1.01	(0.49, 2.11)	
III	65	38	0.83	(0.44, 1.56)	
IV	112	99	2.46	(1.38, 4.4)	
Tumor site					<0.001
Oral	33	25	1.57	(1.01, 2.43)	
Oropharyngeal	30	21	1.39	(0.87, 2.23)	
Laryngohypopharyngeal	156	112	1	-	
Local spread	27	23	2.38	(1.51, 3.75)	
Tumor variant					0.616
Non keratinizing	52	35	1	-	
Keratinizing	194	146	1.1	(0.76, 1.59)	
Microabscesses					0.433
Absent	233	173	1	-	
Present	13	8	0.75	(0.37, 1.53)	
Grade					0.567
G1	41	27	1	-	
G2	154	119	1.22	(0.8, 1.85)	
G3	51	35	1.3	(0.78, 2.15)	
Necrosis in keratinization					0.838
Absent	178	128	1	-	
Present	68	53	1.03	(0.75, 1.43)	
Neutrophils in dyskeratosis					0.507
Absent	120	85	1	-	
Present	126	96	1.10	(0.82, 1.48)	
Tumor necrosis (% of tumor surface)					0.147
Absent	218	158	1	-	
Focal	21	16	1.09	(0.65, 1.83)	
Moderate-extensive	7	7	2.11	(0.98, 4.55)	
Neutrophils in necrosis					0.992
Absent	232	170	1	-	
Present	14	11	1.00	(0.54, 1.85)	
Anaplastic features					0.804
Absent	109	81	1	-	
Present	137	100	0.96	(0.72, 1.29)	

Table IV. Continued.

A, Entire cohort

Parameter	Cases	Events	HR	95% CI	P-value
Cell cannibalism					0.495
Absent	108	79	1	-	
Present	138	102	0.90	(0.67, 1.21)	
Perineural invasion					0.095
Absent	70	47	1	-	
Present	8	7	1.71	(0.9, 3.25)	
Multinucleated macrophages					0.062
Absent	217	164	1	-	
Present	29	17	0.62	(0.37, 1.03)	
Age at 1st diagnosis	246	181	1.01	(1, 1.02)	0.127
Keratin pearls (% of tumor surface)	246	181	1.00	(0.99, 1.02)	0.459
TIL density (%)	240	177	0.99	(0.99, 1)	0.279
Eosinophils/mm^2 average	212	154	1.00	(1, 1)	0.323
CD8$^+$/ mm^2 average	214	157	1.00	(1, 1)	0.184
CD8 heterogeneity					0.030
Homogeneous	118	90	1	-	
Heterogeneous	40	25	0.61	(0.39, 0.96)	

B, Invasive margin

Parameter	Cases	Events	HR	95% CI	P-value
Lymphocytic host response	78	54	0.56	(0.39, 0.81)	0.002
Perineural invasion present	8	7	2.52	(1.12, 5.66)	0.025

Cases refers to the number of patients at the beginning of the study; events refers to the number of patients that developed the event (i.e. died) at the end of the study.

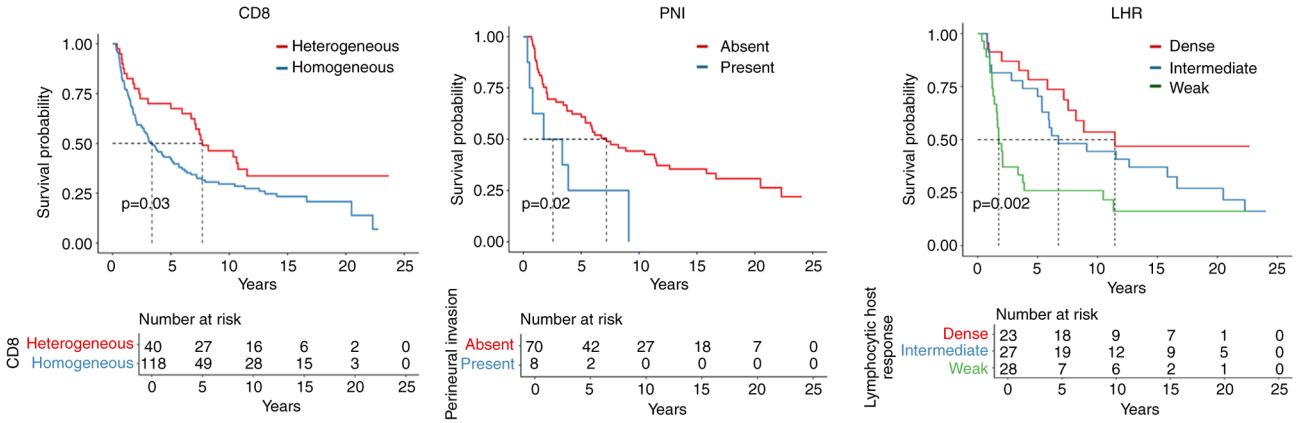

Figure 3. Significant associations of overall survival with CD8 heterogeneity in the entire tumor area as well as with PNI and LHR in the invasive margin. PNI, perineural invasion; LHR, lymphocytic host response.

with OS at a follow-up period of 26 years (24/4/1997-30/11/2023). The results of a univariable analysis are presented in Table IV.

Alcohol consumption and disease stage had significant impacts on patient OS. CD8$^+$ heterogeneity (P=0.038) was associated with a favorable prognosis, whereas perineural invasion in the invasive margin (P=0.025) appeared to be an adverse prognosticator. In addition, weak lymphocytic infiltrates in the invasive margin had a negative impact on OS (Fig. 3).

Table V. Multivariable analysis with respect to OS for the parameters studied in the entire cohort and in the invasive margin.

A, Entire cohort

Parameter	Cases	Events	HR	95% CI	P-value
Alcohol abuse	226	167	1.27	(0.95, 1.7)	0.105
Disease stage	227	168	1.67	(1.11, 2.51)	0.013
Perineural invasion present	8	7	2.81	(1.05, 7.49)	0.039

B, Invasive margin

Parameter	Cases	Events	HR	95% CI	P-value
Lymphocytic host response	80	56	0.58	(0.4, 0.83)	0.003
Perineural invasion present	8	7	2.2	(0.97, 4.98)	0.060

Cases refers to the number of patients at the beginning of the study; events refers to the number of patients that developed the event (i.e. died) at the end of the study.

Table VI. Key histopathological parameters recommended for routine reporting regardless of head and neck squamous cell carcinoma anatomic site.

Category	Parameter	Assessment/reporting
Entire tumour	Histological type[a]	Conventional SCC/other (specify)
	Perineural invasion[a]	Present/absent
	TIL density	% of all stromal mononuclear cells (including lymphocytes and plasma cells)
Invasive front	Lymphocytic host response	Weak/moderate/dense
	Perineural invasion	Present/absent
Immunohistochemistry	p16 immunohistochemistry[a]	Positive/negative
	PD-L1 immunohistochemistry	CPS

[a]Included in current RCPath and CAP core datasets for HNSCC (p16 immunohistochemistry for oropharyngeal SCC).

A subgroup analysis was conducted by separating samples into three distinct groups based on the primary tumor site: oral cavity, oropharynx, and laryngohypopharynx. This additional analysis showed that heavy alcohol abuse and advanced disease stage were significantly associated with worse OS in laryngohypopharyngeal tumors (P<0.001). Furthermore, within the same tumor site, perineural invasion (entire cohort and invasive margin, P=0.007) and weak lymphocytic host response in the invasive margin (P=0.028) were also significantly linked to poorer OS. In oral cavity SCC, weak lymphocytic host response in the invasive margin (P=0.052) was associated with an adverse prognosis. Detailed results of these findings are presented in Tables SI-III and prognostic histological features by site are illustrated in Fig. S2.

A multivariable analysis (Table V) revealed that alcohol abuse, disease stage, and perineural invasion were independently associated with unfavorable OS. In the invasive margin, weak lymphocytic infiltrates and perineural invasion remained independent predictors for unfavorable OS. No additional associations between the clinicopathological parameters studied and OS were observed. Based on these results, we recommend histopathological parameters that should be included, among others, in the histological reports, in each case of HNSCC (Table VI).

Discussion

Grading is one of the primary prognostic factors in malignant neoplasms; however, it does not seem to be an accurate prognosticator for HNSCC, possibly due to the heterogeneity of cytomorphological and architectural features in a pattern previously described as 'hybrid SCC variant' (19). Accordingly, we identified limited areas of keratinization in non-keratinizing tumors and anaplastic cells in otherwise well-differentiated carcinomas. Our observation of heterogeneity beyond neoplastic cells in microenvironmental components, such as stroma and TILs/CD8$^+$ cells, supports the view of HNSCC as heterogeneous ecosystems.

The assessment of routinely reported histological features may assist in developing an optimal prognostic tool in line

with the ongoing effort to establish multifactorial grading systems (5,32). However, we first need to identify which of the histological parameters are risk factors and whether they are site-specific. In this study, as expected, keratinizing tumors exhibited features related to keratinization, and non-keratinizing tumors were mainly characterized as high-grade. Anaplastic features, cell cannibalism, and perineural invasion were observed independent of tumor variant. Comparisons between the SCC of different anatomic locations revealed site-specific characteristics. In oral SCC, high grade was not prevalent, and a common feature was perineural invasion, as previously reported (33). Eosinophil density was higher, as well (34). Necrosis in keratinization, anaplastic cells, and cell cannibalism were mainly present in laryngohypopharyngeal SCC. Interestingly, cell cannibalism and anaplastic features were relatively common in laryngohypopharyngeal SCC, even in low-grade tumors, which is in agreement with previous reports (23). Of note, the literature contains no similar comparative morphological studies based on the HNSCC anatomical site and the observed differences could be used in developing site-specific prognostic profiling tools.

In addition, along the invasive margin, perineural invasion and weak lymphocytic host response were adverse prognosticators independently of the anatomical site. Hence, both parameters should be included in all HNSCC histopathological reporting guidelines, not only in oral carcinomas. Perineural invasion proved to be an independent prognosticator in this study, regardless of nerve diameter and intratumoral localization, in line with previous publications (35,36).

There are ongoing studies focusing on the spatial heterogeneity of the immune cells found in the tumor microenvironment with potential therapeutic implications (37-40). The observed heterogeneity of $CD8^+$ T-cell distribution has been previously mentioned in HNSCC (41,42) without any reference to its prognostic relevance. The association of heterogeneous $CD8^+$ infiltrates with OS described in this paper seems worth further investigation in terms of its therapeutic implications, particularly with respect to immune checkpoint inhibitors. In our series, PD-L1 evaluation showed no significant association with OS, a finding in agreement with previously published data (43). It is emphasized, however, that only a minority of our cases showed PD-L1 positivity, in contrast to former studies (44), raising concerns about its accurate evaluation on TMAs or small biopsy specimens (45).

Recent AI pipelines that fuse histology with genomic data have already achieved prognostic accuracy in other solid tumors (46) and illustrate the potential for similar multimodal models in HNSCC. Digital pathology systems leverage image analysis algorithms and machine learning to identify and quantify microscopic features with greater precision than the standard evaluation (47). Algorithms can be trained to recognize characteristic patterns of LHR-IM and PNI by analyzing H&E-stained slides and even to identify subtle changes in histology, possibly missed by pathologists (48) or to determine the clinical significance of spatial distribution of TILs (49). Machine learning models can be trained on annotated datasets of HNSCC, regarding perineural invasion, the number of nerves, the size of nerves or the different patterns of LHR-IM (48,49). In addition, by using these tools, the interobserver variability is reduced on morphological and immunohistochemical grounds (50), which is crucial with predictive biomarker evaluation, such as PD-L1 CPS. In this context, the performance of these models may exceed that of experienced pathologists.

One of the limitations of this study is the inclusion of both biopsy and surgical material, as well as the accurate representation of histologic characteristics in small biopsy samples. Biopsy material was more common in oropharyngeal tumors. In addition, histological parameters were mainly examined in whole sections, whereas immunohistochemical parameters were examined only on TMA sections. Further, site-specific subgroup analysis for single or profiled parameters in terms of OS was not possible due to the imbalanced respective group sizes. Male predominance may affect the conclusions of this study due to sex-related biological differences. Gender-specific histopathological parameters with potential clinical value weren't investigated and future studies examining sex as a potential modifier of prognostic outcomes in HNSCC are needed. Finally, the lack of HPV-positive tumors should be regarded as an additional limitation.

In conclusion, based on our findings, it seems that the malignant potential of HNSCC is reflected in several tumor biology-related parameters, such as $CD8^+$ spatial heterogeneity, tumor center and/or invasive margin perineural invasion and LHR-IM. Furthermore, perineural invasion and LHR-IM are confirmed as independent histological risk factors in HNSCC. Integrating the above parameters in pathology reports may provide more accurate prognostic information for patients with HNSCC than the routinely assessed histologic grade. The herein presented site-specific and tumor compartment histological parameters may be included in larger studies with deep learning approaches, in order to enable revising histologic grade in HNSCC in a clinically meaningful way, as required in the context of personalized diagnostics.

Acknowledgements

The authors would like to thank Mrs. Maria Moschoni (data coordinator of HeCOG) for administrative support.

Funding

The study is part of the NCR-17-12885 project funded by Astra Zeneca and conducted by HeCOG. It was also partially supported by a Hellenic Society of Medical Oncology (HeSMO) grant (grant no. HE_TR5/25). The funders had no role in study design, data collection and analysis, decision to publish or preparation of the manuscript.

Availability of data and materials

The data generated in the present study may be requested from the corresponding author.

Authors' contributions

SET, VK, GK, PH, GF and TK conceptualized and designed the study, performed the formal analysis and wrote the original draft; KM, SP, KV, SC, AP, PH and GF collected and reviewed clinical and histopathological data. GF and SC confirm the authenticity of all the raw data. All authors have read and approved the final manuscript.

Ethics approval and consent to participate

Written informed consent was obtained from all patients for the use of their data and biological material for research purposes. The protocol was approved by the Bioethics Committee of the Aristotle University of Thessaloniki, School of Health Sciences, Faculty of Medicine (approval no. 5/18.12.2019).

Patient consent for publication

Not applicable.

Competing interests

The authors declare that they have no competing interests.

References

1. Ferlay J, Shin HR, Bray F, Forman D, Mathers C and Parkin DM: Estimates of worldwide burden of cancer in 2008: GLOBOCAN 2008. Int J Cancer 127: 2893-2917, 2010.
2. Ferlay J, Ervik M, Lam F, Colombet M, Mery L, Pineros M, Znaor A, Soerjomataram I and Bray F: Global cancer observatory: Cancer today. International Agency for Research on Cancer, Lyon, France 2020.
3. Johnson DE, Burtness B, Leemans CR, Lui VWY, Bauman JE and Grandis JR: Head and neck squamous cell carcinoma. Nat Rev Dis Primers 6: 92, 2020.
4. Aupérin A: Epidemiology of head and neck cancers: An update. Curr Opin Oncol 32: 178-186, 2020.
5. El-Naggar AK, Chan JKC, Grandis JR, Takata T and Slootweg PJ: WHO classification of head and neck tumours. International Agency for Research on Cancer2017.
6. Lewis JS Jr, Beadle B, Bishop JA, Chernock RD, Colasacco C, Lacchetti C, Moncur JT, Rocco JW, Schwartz MR, Seethala RR, *et al*: Human papillomavirus testing in head and neck carcinomas: Guideline from the college of american pathologists. Arch Pathol Lab Med 142: 559-597, 2018.
7. World Health Organization (WHO): WHO Classification of Head and Neck Tumors, 2023.
8. National Comprehensive Cancer Network (NCCN): NCCN Clinical Practice Guidelines in Oncology: Head and Neck Cancers, 2025.
9. Liu FL, Zhang ZC, Zhou SL, Liu XL and Xu W: Unlocking the therapeutic potential of LncRNA BLACAT1 in hypopharynx squamous cell carcinoma. Discov Med 36: 546-558, 2024.
10. Liu Z, Zhao Z, Xie L, Xiao Z, Li M, Li Y and Luo T: Proteomic analysis reveals chromatin remodeling as a potential therapeutical target in neuroblastoma. J Transl Med 23: 234, 2025.
11. Elmusrati A, Wang J and Wang CY: Tumor microenvironment and immune evasion in head and neck squamous cell carcinoma. Int J Oral Sci 13: 24, 2021.
12. Bryne M, Jenssen N and Boysen M: Histological grading in the deep invasive front of T1 and T2 glottic squamous cell carcinomas has high prognostic value. Virch Arch 427: 277-281, 1995.
13. Brandwein-Gensler M, Smith RV, Wang B, Penner C, Theilken A, Broughel D, Schiff B, Owen RP, Smith J, Sarta C, *et al*: Validation of the histologic risk model in a new cohort of patients with head and neck squamous cell carcinoma. Am J Surg Pathol 34: 676-688, 2010.
14. Fountzilas G, Ciuleanu E, Bobos M, Kalogera-Fountzila A, Eleftheraki AG, Karayannopoulou G, Zaramboukas T, Nikolaou A, Markou K, Resiga L, *et al*: Induction chemotherapy followed by concomitant radiotherapy and weekly cisplatin versus the same concomitant chemoradiotherapy in patients with nasopharyngeal carcinoma: A randomized phase II study conducted by the hellenic cooperative oncology group (HeCOG) with biomarker evaluation. Ann Oncol 23: 427-435, 2012.
15. Krikelis D, Bobos M, Karayannopoulou G, Resiga L, Chrysafi S, Samantas E, Andreopoulos D, Vassiliou V, Ciuleanu E and Fountzilas G: Expression profiling of 21 biomolecules in locally advanced nasopharyngeal carcinomas of Caucasian patients. BMC Clin Pathol 13: 1, 2013.
16. Fountzilas G, Psyrri A, Giannoulatou E, Tikas I, Manousou K, Rontogianni D, Ciuleanu E, Ciuleanu T, Resiga L, Zaramboukas T, *et al*: Prevalent somatic BRCA1 mutations shape clinically relevant genomic patterns of nasopharyngeal carcinoma in Southeast Europe. Int J Cancer 142: 66-80, 2018.
17. Hendry S, Salgado R, Gevaert T, Russell PA, John T, Thapa B, Christie M, van de Vijver K, Estrada MV, Gonzalez-Ericsson PI, *et al*: Assessing tumor-infiltrating lymphocytes in solid tumors: A practical review for pathologists and proposal for a standardized method from the international immunooncology biomarkers working group: Part 1: Assessing the host immune response, TILs in invasive breast carcinoma and ductal carcinoma in situ, metastatic tumor deposits and areas for further research. Adv Anat Pathol 24: 235-251, 2017.
18. Zhang D, He W, Wu C, Tan Y, He Y, Xu B, Chen L, Li Q and Jiang J: Scoring system for tumor-infiltrating lymphocytes and its prognostic value for gastric cancer. Front Immunol 10: 71, 2019.
19. Chernock RD: Morphologic features of conventional squamous cell carcinoma of the oropharynx: 'Keratinizing' and 'nonkeratinizing' histologic types as the basis for a consistent classification system. Head Neck Pathol 6 (Suppl 1): S41-S47, 2012.
20. Amin MB, Edge SB, Greene FL, Byrd DR, Brookland RK, Washington MK, Gershenwald JE, Compton CC, Hess KR, Sullivan DC, *et al*: AJCC Cancer Staging Manual. 8th Edition, Springer International Publishing, Cham, Switzerland, pp 91-156, 2018.
21. Pollheimer MJ, Kornprat P, Lindtner RA, Harbaum L, Schlemmer A, Rehak P and Langner C: Tumor necrosis is a new promising prognostic factor in colorectal cancer. Human Pathol 41: 1749-1757, 2010.
22. Kumar V, Abbas AK, Aster JC and Perkins JA: Robbins basic pathology. 10th Edition, Elsevier, Amsterdam, Netherlands, pp 193, 2017.
23. Almangush A, Mäkitie AA, Hagström J, Haglund C, Kowalski LP, Nieminen P, Coletta RD, Salo T and Leivo I: Cell-in-cell phenomenon associates with aggressive characteristics and cancer-related mortality in early oral tongue cancer. BMC Cancer 20: 843, 2020.
24. Jiang Z, Chen Z, Xu Y, Li H, Li Y, Peng L, Shan H, Liu X, Wu H, Wu L, *et al*: Low-frequency ultrasound sensitive piezo1 channels regulate keloid-related characteristics of fibroblasts. Adv Sci 11: e2305489, 2024.
25. Ueno H, Kanemitsu Y, Sekine S, Ishiguro M, Ito E, Hashiguchi Y, Kondo F, Shimazaki H, Mochizuki S, Kajiwara Y, *et al*: Desmoplastic pattern at the tumor front defines poor-prognosis subtypes of colorectal cancer. Am J Surg Pathol 41: 1506-1512, 2017.
26. Salgado R, Denkert C, Demaria S, Sirtaine N, Klauschen F, Pruneri G, Wienert S, Van den Eynden G, Baehner FL, Penault-Llorca F, *et al*: The evaluation of tumor-infiltrating lymphocytes (TILs) in breast cancer: Recommendations by an international TILs working group 2014. Ann Oncol 26: 259-271, 2015.
27. Hendry S, Salgado R, Gevaert T, Russell PA, John T, Thapa B, Christie M, van de Vijver K, Estrada MV, Gonzalez-Ericsson PI, *et al*: Assessing tumor-infiltrating lymphocytes in solid tumors: A practical review for pathologists and proposal for a standardized method from the international immuno-oncology biomarkers working group: Part 2: TILs in melanoma, gastrointestinal tract carcinomas, non-small cell lung carcinoma and mesothelioma, endometrial and ovarian carcinomas, squamous cell carcinoma of the head and neck, genitourinary carcinomas, and primary brain tumors. Adv Anat Pathol 24: 311-335, 2017.
28. Koletsa T, Kotoula V, Koliou GA, Manousou K, Chrisafi S, Zagouri F, Sotiropoulou M, Pentheroudakis G, Papoudou-Bai A, Christodoulou C, *et al*: Prognostic impact of stromal and intratumoral CD3, CD8 and FOXP3 in adjuvantly treated breast cancer: Do they add information over stromal tumor-infiltrating lymphocyte density? Cancer Immunol Immunother 69: 1549-1564, 2020.
29. Brandwein-Gensler M, Teixeira MS, Lewis CM, Lee B, Rolnitzky L, Hille JJ, Genden E, Urken ML and Wang BY: Oral squamous cell carcinoma: Histologic risk assessment, but not margin status, is strongly predictive of local disease-free and overall survival. Am J Surg Pathol 29: 167-178, 2005.
30. Agilent Technologies Inc.: PD-L1 IHC 22C3 pharmDx Interpretation Manual-Head and Neck Squamous Cell Carcinoma (HNSCC). Santa Clara, CA, USA, pp 1-72. https://www.agilent.com/cs/library/usermanuals/public/29314_22c3_pharmDx_hnscc_interpretation_manual_us.pdf. Accessed April 2, 2024.

31. Seethala RR, Baras A, Baskovich BW, Birdsong GG, Fitzgibbons PL, Khoury JD, Schneider F: Head and Neck Biomarker Reporting Template. Version 2.0.0.0. College of American Patologists, pp 1-6, 2021.
32. Almangush A, Mäkitie AA, Triantafyllou A, de Bree R, Strojan P, Rinaldo A, Hernandez-Prera JC, Suárez C, Kowalski LP, Ferlito A and Leivo I: Staging and grading of oral squamous cell carcinoma: An update. Oral Oncol 107: 104799, 2020.
33. Schmitd LB, Scanlon CS and D'Silva NJ: Perineural invasion in head and neck cancer. J Dental Res 97: 742-750, 2018.
34. Sharma HD, Mahadesh J, Monalisa W, Gopinathan PA, Laxmidevi BL and Sanjenbam N: Quantitative assessment of tumor-associated tissue eosinophilia and nuclear organizing region activity to validate the significance of the pattern of invasion in oral squamous cell carcinoma: A retrospective study. J Oral Maxillofac Pathol 25: 258-265, 2021.
35. Binmadi N, Alsharif M, Almazrooa S, Aljohani S, Akeel S, Osailan S, Shahzad M, Elias W and Mair Y: Perineural invasion is a significant prognostic factor in oral squamous cell carcinoma: A systematic review and meta-analysis. Diagnostics (Basel) 13: 3339, 2023.
36. Huang Q, Huang Y, Chen C, Zhang Y, Zhou J, Xie C, Lu M, Xiong Y, Fang D, Yang Y, *et al*: Prognostic impact of lymphovascular and perineural invasion in squamous cell carcinoma of the tongue. Sci Rep 13: 3828, 2023.
37. Yuan Y: Spatial heterogeneity in the tumor microenvironment. Cold Spring Harb Perspect Med 6: a026583, 2016.
38. Galon J, Mlecnik B, Bindea G, Angell HK, Berger A, Lagorce C, Lugli A, Zlobec I, Hartmann A, Bifulco C, *et al*: Towards the introduction of the 'Immunoscore' in the classification of malignant tumours. J Pathol 232: 199-209, 2014.
39. Zhang XM, Song LJ, Shen J, Yue H, Han YQ, Yang CL, Liu SY, Deng JW, Jiang Y, Fu GH, *et al*: Prognostic and predictive values of immune infiltrate in patients with head and neck squamous cell carcinoma. Hum Pathol 82: 104-112, 2018.
40. Almangush A, De Keukeleire S, Rottey S, Ferdinande L, Vermassen T, Leivo I and Mäkitie AA: Tumor-infiltrating lymphocytes in head and neck cancer: Ready for prime time? Cancers (Basel) 14: 1558, 2022.
41. Balermpas P, Michel Y, Wagenblast J, Seitz O, Weiss C, Rödel F, Rödel C and Fokas E: Tumour-infiltrating lymphocytes predict response to definitive chemoradiotherapy in head and neck cancer. Br J Cancer 110: 501-509, 2014.
42. Chatzopoulos K, Kotoula V, Manoussou K, Markou K, Vlachtsis K, Angouridakis N, Nikolaou A, Vassilakopoulou M, Psyrri A and Fountzilas G: Tumor infiltrating lymphocytes and CD8+ T cell subsets as prognostic markers in patients with surgically treated laryngeal squamous cell carcinoma. Head Neck Pathol 14: 689-700, 2020.
43. Yang WF, Wong MCM, Thomson PJ, Li KY and Su YX: The prognostic role of PD-L1 expression for survival in head and neck squamous cell carcinoma: A systematic review and meta-analysis. Oral Oncol 86: 81-90, 2018.
44. Crosta S, Boldorini R, Bono F, Brambilla V, Dainese E, Fusco N, Gianatti A, L'Imperio V, Morbini P and Pagni F: PD-L1 testing and squamous cell carcinoma of the head and neck: A multicenter study on the diagnostic reproducibility of different protocols. Cancers (Basel) 13: 292, 2021.
45. De Keukeleire SJ, Vermassen T, Deron P, Huvenne W, Duprez F, Creytens D, Van Dorpe J, Ferdinande L and Rottey S: Concordance, correlation, and clinical impact of standardized PD-L1 and TIL scoring in SCCHN. Cancers (Basel) 14: 2431, 2022.
46. He B, Wang L, Zhou W, Liu H, Wang Y, Lv K and He K: A fusion model to predict the survival of colorectal cancer based on histopathological image and gene mutation. Sci Rep 15: 9677, 2025.
47. Baxi V, Edwards R, Montalto M and Saha S: Digital pathology and artificial intelligence in translational medicine and clinical practice. Mod Pathol 35: 23-32, 2022.
48. Lee LY, Yang CH, Lin YC, Hsieh YH, Chen YA, Chang MD, Lin YY and Liao CT: A domain knowledge enhanced yield based deep learning classifier identifies perineural invasion in oral cavity squamous cell carcinoma. Front Oncol 12: 951560, 2022.
49. Abousamra S, Gupta R, Hou L, Batiste R, Zhao T, Shankar A, Rao A, Chen C, Samaras D, Kurc T and Saltz J: Deep learning-based mapping of tumor infiltrating lymphocytes in whole slide images of 23 types of cancer. Front Oncol 11: 806603, 2021.
50. Badve S, Kumar GL, Lang T, Peigin E, Pratt J, Anders R, Chatterjee D, Gonzalez RS, Graham RP, Krasinskas AM, *et al*: Augmented reality microscopy to bridge trust between AI and pathologists. NPJ Precis Oncol 9: 139, 2025.